**Rheologica Acta** Rheol Acta 32:227–244 (1993)

# Orientation tensors in simple flows of dilute suspensions of non-Brownian rigid ellipsoids, comparison of analytical and approximate solutions

M. C. Altan and L. Tang

School of Aerospace and Mechanical Engineering, University of Oklahoma, Norman, Oklahoma, USA

*Abstract:* General analytical solutions are obtained for the planar orientation structure of rigid ellipsoid of revolutions subjected to an arbitrary homogeneous flow in a Newtonian fluid. Both finite and infinite aspect ratio particles are considered. The orientation structure is described in terms of two-dimensional, time-dependent tensors that are commonly employed in constitutive equations for anisotropic fluids such as fiber suspensions. The effect of particle aspect ratio on the evolution of orientation structure is studied in simple shear and planar elongational flows. With the availability of analytical solutions, accuracies of quadratic closure approximations used for nonhomogeneous flows are analyzed, avoiding numerical integration of orientation distribution function. In general, fourth-order orientation evolution equations with sixth-order quadratic closure approximations yield more accurate representations compared to the commonly used second-order evolution equations with fourth-order quadratic closure approximations. However, quadratic closure approximations of any order are found to give correct maximum orientation angle (i.e., preferred direction) results for all particle aspect ratios and flow cases.

*Key words:* Fiber suspensions – orientation tensors – closure equations

## 1. Introduction

Flows containing small elongated particles are encountered in a number of engineering and biological systems. Such material systems usually exhibit unique rheological behavior depending on the particle concentration and other geometrical parameters. The rheological characterization and constitutive modeling of particle suspensions have caught the attention of several researchers. Consequently, numerous constitutive models have been proposed which combine microstructural information with continuum representation (Ericksen, 1960; Batchelor, 1970; Hinch and Leal, 1975, 1976; Evans, 1975; Dinh and Armstrong, 1984; Phan-Thien and Graham, 1991).

In general, bulk stress tensor for the dilute suspensions containing neutrally buoyant, non-Brownian rigid ellipsoids of revolution is expressed as

$$\sigma_{ij} = \sigma^f_{ij} + \sigma^p_{ij}$$

$$\sigma^f_{ij} = \mu(u_{ij} + u_{ji}) \tag{1}$$

$$\sigma^p_{ij} = \mu\phi_v(A\,S_{ijkl}u_{kl} + B[S_{ik}u_{kj} + u_{ik}S_{kj}] + Cu_{ij}) \ ,$$

where $\sigma^f_{ij}$ and $\sigma^p_{ij}$ are the stress contributions from the suspending fluid and the particles, respectively, $u_{ij}$ is the velocity gradient tensor, $\phi_v$ is the particle volume fraction, $S_{ij}$ and $S_{ijkl}$ are the second- and fourth-order orientation tensors which describe the orientation structure, and $A$, $B$, $C$ are the material constants that depend on the particle geometry. A brief discussion of various constitutive models and explicit expressions for the material constants $A$, $B$, and $C$ can be found in Altan (1990) and Tucker (1991).

Orientation tensors $S_{ij}$ and $S_{ijkl}$ are defined as the second- and fourth-order moments of the orientation distribution function, and relate rheological properties to fluid kinematics. Obviously, using tensorial quantities provides a concise and convenient way to describe the orientation field. For nonhomogeneous flow[1]) of suspensions where the velocity gradient tensor is not spatially uniform, Eq. (1) should be used

[1]) In this paper, the term homogeneous flow is used to describe flows with spatially constant velocity gradient tensor. For such flows, the term linear flow is also used by some researchers.

with Cauchy momentum equations for the solution of flow kinematics. In addition, simultaneous solution of the orientation evolution equations is also needed for the characterization of orientation field. A few numerical solutions of this coupled problem have recently been reported (Papanastasiou and Alexandrou, 1987; Lipscomb et al., 1988; Chiba et al., 1990; Rosenberg et al., 1990; Altan et al., 1992; Lee, 1992). The common practice is to calculate the orientation tensors directly from flow kinematics by solving a set of coupled differential equations. However, the resulting orientation evolution equations generate a classical closure problem. Different types of closure approximations are proposed and investigated by several researchers (Hand, 1960; Hinch and Leal, 1976; Doi, 1981; Advani and Tucker, 1987, 1990; Altan et al., 1989; Maffettone and Marucci, 1991). The ad-hoc application of such closure approximations are found to introduce considerable numerical error despite their computational convenience.

Another approach that avoids using closure approximations is suggested by Papanastasiou and Alexandrou (1987) and applied to a constitutive model for non-dilute fiber suspensions proposed by Dinh and Armstrong (1984). This approach evaluates the orientation state from the deformation gradient tensor of the fluid calculated along the fiber pathlines, and so far has only been implemented for infinite aspect ratio fibers. The solution of deformation gradient equations may present a viable choice for fiber suspensions; however, as in the case of other deformation-dependent constitutive equations, the numerical accumulation of errors at large deformation values needs to be investigated further (Keunings, 1989). More recently, the theoretical basis of a similar technique is presented by Szeri and Leal (1992) which also proposes the implementation of the Lagrangian description in both flow and orientation spaces.

It should be noted that, at relatively low particle concentrations, the particle stress contribution $\sigma_{ij}^{p}$ is linearly related with particle volume fraction $\phi_v$ as Eq. (1) indicates. Therefore, the particle stress contribution linearly vanishes for the zero volume fraction limit. Corollary to this, one can conclude that for a complex suspension flow where the velocity gradient tensor is spatially non-uniform, there exists a critical particle volume fraction below which the material system behaves like a Newtonian fluid. However, even if the flow kinematics is not affected by the presence of particles at such low volume fractions, the accurate determination of orientation structure in complex flows is of extreme importance. The orientation solutions for such cases (i.e., zero-volume-fraction-limit solutions) provide valuable insight regarding the suspension behavior and fluid-particle interactions of very dilute systems.

In this paper, after a brief introduction of theoretical basics, the analytical expressions for the evolution of the second- and fourth-order orientation tensors of a two-dimensional (i.e., planar) orientation structure subjected to an arbitrary homogeneous flow are presented. With the availability of analytical expressions, accuracies of commonly used quadratic closure approximations are analyzed. Particularly, the following three important questions are investigated regarding the closure approximations.

1) Do higher order (i.e., sixth-order) closure approximations always yield more accurate results compared to lower order (i.e., fourth-order) approximations?

2) Are there special conditions where fourth-order quadratic approximation fails completely and should not be used?

3) Can any orientation parameter be correctly predicted by lower order evolution equations?

In the last part of this paper, a simple channel flow example is presented. The analytical $S_{ij}$ results, depicted by orientation ellipses, are compared with the $S_{ij}$ values obtained by both second- and fourth-order orientation evolution equations.

## 2. Theory

### *2.1 Description of orientation state*

#### *2.1.1 Orientation vector*

The orientation of an ellipsoid of revolution suspended in a Newtonian fluid can be specified by a unit vector. The orientation vector $\vec{p}$ coincides with the major axis of the ellipsoid of revolution and rotates with the bulk fluid deformation. The motion of a rigid, neutrally buoyant, ellipsoidal particle in homogeneous flows is first studied by Jeffrey (1922). For such flows, the time rate of change of the orientation vector of an ellipsoid of revolution can be expressed as

$$\dot{p}_i = (\Omega_{ij} + \lambda \Delta_{ij}) p_j - \lambda p_i p_l p_k \Delta_{lk} \ , \qquad (2)$$

where $\Omega_{ij}$ and $\Delta_{ij}$ are the vorticity and strain rate tensors, respectively.

$$\Omega_{ij} = \frac{1}{2}\left(\frac{\partial u_i}{\partial x_j} - \frac{\partial u_j}{\partial x_i}\right) \quad (3)$$
$$\Delta_{ij} = \frac{1}{2}\left(\frac{\partial u_i}{\partial x_j} + \frac{\partial u_j}{\partial x_i}\right)$$

$$\lambda = \frac{a_p^2 - 1}{a_p^2 + 1} \quad . \quad (4)$$

In the above equations, $i,j = 1,2$, and summation is implied over repeated indices. The parameter $\lambda$ is a function of the particle aspect ratio $a_p$, which is defined as the length to diameter ratio of the particle. The ellipsoid of revolutions, with two equal principal axes, can be classified as oblate or prolate spheroids. For oblate spheroids, the equal axes are larger than the third axis. Therefore, $a_p = l/d < 1$, and $-1 \leq \lambda < 0$. For prolate spheroids, the equal axes are smaller than the third one. Therefore, $a_p = l/d > 1$, and $0 < \lambda \leq 1$. In this study, the analysis will be limited to prolate spheroids which will be referred to as fibers.

The rheological behavior of non-dilute systems (i.e., $\phi_v a_p^2 > 1$) may not be fully described by the constitutive equation expressed in Eq. (1) and by the Jeffrey's equation given in Eq. (2) since the interactions between fibers are not accounted for. Hence, for such cases, different forms and extensions of Jeffrey's equation are proposed. One approach is to include an additional term in Jeffrey's equation similar to the Brownian diffusion term used for microscopic particles. Such extensions to Jeffrey's equation are experimentally observed to be useful in simulating the interactions between particles for non-dilute systems (Folgar and Tucker, 1984; Stover et al., 1992). Nevertheless, even for non-dilute systems with $\phi_v a_p^2 \approx 50$, the deviation of particle rotations from Jeffrey's orbits are observed to be rather small. Therefore, one may expect that the validity of Eq. (1) and Eq. (2) to extend over non-dilute suspensions with minor modifications (Phan-Thien and Graham, 1991).

### 2.1.2 Orientation distribution function

The orientation distribution function $\Psi(\vec{p},t)$ provides a complete representation of the fiber orientation state. It gives the probability of having a fiber at a certain orientation $\vec{p}$ at time $t$. Equivalently, it can also be defined in terms of the orientation angle as the probability of finding a fiber within a certain angular interval specified by $\phi_1$ and $\phi_2$ at time $t$.

For two-dimensional representation of fiber orientation state, the orientation distribution function should satisfy certain conditions. Since one end of a fiber is not distinguishable from the other, the distribution function has a period of $\pi$, or

$$\Psi(\phi) = \Psi(\phi + \pi) \quad . \quad (5)$$

In addition, the normalization condition is satisfied, implying that the area under a distribution function curve is always unity.

$$\int_0^{\pi} \Psi(\phi)\, d\phi = 1 \quad . \quad (6)$$

The orientation distribution function can be determined by solving the governing partial differential equation expressed as

$$\frac{\partial \Psi(\vec{p},t)}{\partial t} = -\frac{\partial [\dot{p}_i \Psi(\vec{p},t)]}{\partial p_i} \quad , \quad (7)$$

where $\dot{p}_i$ is given by Eq. (2). The governing equation for orientation distribution function is a form of the Fokker-Planck equation used for homogeneous flows with negligible Brownian motion.

### 2.1.3 Orientation tensors

Orientation state of fibers in a suspension can also be described with reasonable accuracy with tensors. A number of researchers have used orientation tensors successfully for the numerical computation of fiber orientation (Lipscomb et al., 1987; Altan et al., 1990; Lee, 1992) and for the representation of rheological properties of fiber suspensions (Altan et al., 1989; Malamataris and Papanastasiou, 1991). The second- and fourth-order (i.e., $S_{ij}$ and $S_{ijkl}$, respectively) orientation tensors are defined as

$$S_{ij} = \langle p_i p_j \rangle = \int p_i p_j \Psi(\vec{p})\, d\vec{p}$$
$$S_{ijkl} = \langle p_i p_j p_k p_l \rangle = \int p_i p_j p_k p_l \Psi(\vec{p})\, d\vec{p} \quad . \quad (8)$$

The order of the indices is not important since the orientation tensors are completely symmetric. An important property of orientation tensors is that the higher order tensors contain the lower order ones (i.e., the lower order orientation tensors can be written in terms of the higher order orientation tensors). For example, any second-order tensor component can be written in terms of fourth-order components as

$$S_{ij} = S_{ijkk} \ . \tag{9}$$

It can also be shown that the trace of the second-order tensor is unity.

$$S_{ii} = 1 \ . \tag{10}$$

The eigenvectors and eigenvalues of the second-order tensor indicate the maximum orientation direction and the degree of alignment with respect to that direction, respectively. Hence, the preferred orientation angle can be easily computed from the components of the second-order orientation tensor.

*2.2 Analytical solutions of orientation tensors*

As shown by Bretherton (1962), it is possible to obtain analytical solution of Eq. (2), which would specify the rotation of non-Brownian rigid ellipsoid of revolutions suspended in an arbitrary two- or three-dimensional homogeneous flow. Specifically, explicit analytical expressions for planar particle rotation have been obtained for arbitrary two-dimensional homogeneous flows. In addition, three-dimensional particle rotation in some of the simple flows has been well characterized.

Following Bretherton's work, the solution of Eq. (2) with the initial condition $p_i = p_i^0$ has been shown to be

$$p_i = \frac{E_{il} p_l^0}{(E_{lm} E_{lj} p_j^0 p_m^0)^{1/2}} \ , \tag{11}$$

where $E_{ij}$ is the particle rotation tensor and defined as

$$\frac{dE_{ij}}{dt} = (\Omega_{ik} + \lambda \Delta_{ik}) E_{kj} \tag{12}$$

with the initial condition $E = I$ (unit tensor).

This representation is valid for both two- and three-dimensional orientations and flow fields. For infinite aspect ratio particles (i.e., slender bodies with $\lambda = 1$), the particle rotation tensor $E_{ij}$ becomes the actual strain tensor of the flow field and is defined as

$$E_{ij} = \frac{\partial x_i}{\partial x_j^0} \ , \tag{13}$$

where $x_i$ and $x_j^0$ are the fluid particle coordinates at times $t$ and $t^0$, respectively.

For any two-dimensional homogeneous flow, the velocity gradient tensor can be specified as

$$u_{ij} = \begin{bmatrix} \frac{\partial u_1}{\partial x_1} & \frac{\partial u_1}{\partial x_2} \\ \frac{\partial u_2}{\partial x_1} & \frac{\partial u_2}{\partial x_2} \end{bmatrix} = \begin{pmatrix} c & c_1 \\ c_2 & -c \end{pmatrix} \ , \tag{14}$$

where $c$, $c_1$, and $c_2$ are arbitrary constants, and the trace of $u_{ij}$ should be zero to satisfy the conservation of mass for incompressible flow. A single parameter $w^2$ can be utilized to define the solution families of Eq. (12) with an arbitrary velocity gradient tensor.

$$w^2 = \frac{\lambda^2 (B^2 + 4c^2) - A^2}{4} \ , \tag{15}$$

where $B = c_1 + c_2$ and $A = c_1 - c_2$. Depending on the value of $w^2$, three different solution families are possible as shown by Akbar and Altan (1992).

When $w^2 = 0$,

$$E_{ij} = \begin{bmatrix} 1 + \lambda ct & \frac{(\lambda B + A)t}{2} \\ \frac{(\lambda B - A)t}{2} & 1 - \lambda ct \end{bmatrix} \ . \tag{16}$$

When $w^2 > 0$,

$$E_{ij} = \begin{bmatrix} \frac{w\cosh(wt) + \lambda c \sinh(wt)}{w} & \frac{(\lambda B + A)\sinh(wt)}{2w} \\ \frac{(\lambda B - A)\sinh(wt)}{2w} & \frac{w\cosh(wt) - \lambda c \sinh(wt)}{w} \end{bmatrix} \ . \tag{17}$$

When $w^2 < 0$,

$$E_{ij} = \begin{bmatrix} \frac{w\cos(wt) + \lambda c \sin(wt)}{w} & \frac{(\lambda B + A)\sin(wt)}{2w} \\ \frac{(\lambda B - A)\sin(wt)}{2w} & \frac{w\cos(wt) - \lambda c \sin(wt)}{w} \end{bmatrix} \ , \tag{18}$$

where in Eq. (18) $w$ is defined as $w = \sqrt{|w^2|}$. Equations (16) – (18) are the possible solutions for particle rotation tensor and can be used in Eq. (11) to specify the rotation of both oblate and prolate spheroids subjected to an arbitrary homogeneous flow. Although it is straightforward to use Eqs. (16) – (18) for three-dimensional orientation vectors, in this paper the

analysis will be limited to planar orientations. For infinite aspect ratio fibers where $\lambda = 1$, Eqs. (16) – (18) simplify such that the three $E_{ij}$'s represent actual strain tensors for the simple shear, extensional, and rotational flows, respectively.

The particle rotation tensors can also be determined for three-dimensional homogeneous flows from Eq. (12). The resulting equations can be grouped into three with each one containing three coupled differential equations. The analytical solutions of these three sets of equations can be obtained, characterizing the particle rotation in general three-dimensional homogeneous flows.

If the initial distribution of particle orientation is known, the time-dependent evolution of orientation distribution function can be obtained analytically. For planar orientations, using normalization condition as given in Eq. (6), the initial condition for randomly oriented particles becomes

$$\Psi(\vec{p}, t=0) = \frac{1}{\pi} \ . \tag{19}$$

Therefore, for random initial condition, the solution of Eq. (7) with Eq. (2) can be expressed as

$$\Psi(\vec{p}, t) = \frac{1}{\pi} (\Lambda_{lm}\Lambda_{lj}p_j p_m)^{-1} \ , \tag{20}$$

where $\Lambda_{ij}$ is the inverse of particle rotation tensor $E_{ij}$. Equation (20) can be rearranged by using planar orientation angle $\phi$ as

$$\Psi(\phi, t) = \frac{1}{\pi}\left(a_1 \cos^2\phi + \frac{1}{2}a_2 \sin 2\phi + a_3 \sin^2\phi\right)^{-1} , \tag{21}$$

where

$$\begin{aligned} a_1 &= \Lambda_{11}^2 + \Lambda_{21}^2 \\ a_2 &= 2(\Lambda_{11}\Lambda_{12} + \Lambda_{21}\Lambda_{22}) \\ a_3 &= \Lambda_{12}^2 + \Lambda_{22}^2 \ . \end{aligned} \tag{22}$$

Determining analytical solutions of the second- and fourth-order orientation tensors involves calculation of the integrals given by Eq. (8). For the second-order orientation tensor $S_{ij}$, the resulting integral becomes

$$S_{ij} = \frac{1}{\pi}\int_0^{\pi} \frac{\cos^{(4-\xi)}\phi \sin^{(\xi-2)}\phi}{a_1\cos^2\phi + \frac{1}{2}a_2 \sin 2\phi + a_3 \sin^2\phi} d\phi \ , \tag{23}$$

where $\xi = i+j$. Similarly, the fourth-order orientation tensor $S_{ijkl}$ can be expressed as

$$S_{ijlk} = \frac{1}{\pi}\int_0^{\pi} \frac{\cos^{(8-\xi)}\phi \sin^{(\xi-4)}\phi}{a_1\cos^2\phi + \frac{1}{2}a_2 \sin 2\phi + a_3 \sin^2\phi} d\phi \ , \tag{24}$$

where $\xi = i+j+k+l$. The integrals given in Eqs. (23) – (24) can be evaluated with the transformation $x = \tan\phi$.

Consequently, the $S_{ij}$ components are obtained as

$$S_{11} = \frac{1}{2}\frac{a_2^2 - 2(a_3 - a_1)(1 - a_3)}{(a_1 - a_3)^2 + a_2^2} \tag{25}$$

$$S_{12} = \frac{1}{2}\frac{2a_2 - a_2(a_1 - a_3)}{(a_1 - a_3)^2 + a_2^2} \tag{26}$$

$$S_{22} = \frac{1}{2}\frac{a_2^2 + 2(a_3 - a_1)(1 - a_1)}{(a_1 - a_3)^2 + a_2^2} \ . \tag{27}$$

From Eq. (24), the $S_{ijkl}$ components become

$$\begin{aligned} S_{1111} = {} & \frac{(a_1 - 3a_3)[(a_1 - a_3)^2 - a_2^2] + 4a_2^2(a_1 - a_3)}{2[(a_1 - a_3)^2 + a_2^2]^2} \\ & + \frac{2a_3^4 + 2a_3^2a_2^2 + d_2^4 - 4a_1a_3^3 - 4a_1a_2^2a_3 + 2a_1^2a_3^2}{\sqrt{4a_1a_3 - a_2^2}\,[(a_1 - a_3)^2 + a_2^2]^2} \end{aligned} \tag{28}$$

$$\begin{aligned} S_{1112} = {} & -\frac{4a_3a_2(a_1 - a_3) + a_2[(a_1 - a_3)^2 - a_2^2]}{2[(a_1 - a_3)^2 + a_2^2]^2} \\ & + \frac{a_2(3a_1^2a_3 - a_1a_2^2 - 2a_1a_3^2 - a_3^3)}{\sqrt{4a_1a_3 - a_2^2}\,[(a_1 - a_3)^2 + a_2^2]^2} \end{aligned} \tag{29}$$

$$\begin{aligned} S_{1122} = {} & \frac{(a_1 + a_3)[(a_1 - a_3)^2 - a_2^2]}{2[(a_1 - a_3)^2 + a_2^2]^2} \\ & + \frac{a_3^2a_2^2 - 2a_1a_3^3 + 4a_1^2a_3^2 + a_1^2a_2^2 - 2a_1^3a_3}{\sqrt{4a_1a_3 - a_2^2}\,[(a_1 - a_3)^2 + a_2^2]^2} \end{aligned} \tag{30}$$

$$\begin{aligned} S_{1222} = {} & \frac{a_2[-(a_1 - a_3)^2 + a_2^2] + 4a_1a_2(a_1 - a_3)}{2[(a_1 - a_3)^2 + a_2^2]^2} \\ & + \frac{a_2[3a_1a_3^2 - a_1^3 - 2a_1^2a_3 - a_2^2a_3]}{\sqrt{4a_1a_3 - a_2^2}\,[(a_1 - a_3)^2 + a_2^2]^2} \end{aligned} \tag{31}$$

$$S_{2222} = \frac{(a_3 - 3a_1)[(a_1 - a_3)^2 - a_2^2] - 4a_2^2(a_1 - a_3)}{2[(a_1 - a_3)^2 + a_2^2]^2} + \frac{a_2^4 - 4a_1a_2^2a_3 + 2a_1^2a_2^2 + 2a_1^2a_3^2 + 2d_1^4 - 4a_1^3a_3}{\sqrt{4a_1a_3 - a_2^2}\,[(a_1 - a_3)^2 + a_2^2]^2} . \quad (32)$$

### 2.2.1 Simple shear flow

The velocity gradient tensor for a simple shear flow is expressed as

$$u_{ij} = \begin{pmatrix} 0 & c_1 \\ 0 & 0 \end{pmatrix} , \quad (33)$$

where $c_1$ represents the shear rate. It can be easily seen that $w^2$, defined in Eq. (15), becomes

$$w^2 = \frac{c_1^2(\lambda^2 - 1)}{4} . \quad (34)$$

Since $\lambda^2 < 1$ for finite aspect ratio particles, $w^2 < 0$. Therefore, the second- and fourth-order orientation tensor components for the simple shear flow simplify as

$$S_{11} = \frac{a_1 + a_1a_3 - a_3 + a_3^2 - 2}{(a_1 + a_3)^2 - 4} \quad (35)$$

$$S_{12} = \frac{a_2(2 - a_1 - a_3)}{2[(a_1 + a_3)^2 - 4]} \quad (36)$$

$$S_{22} = \frac{a_1^2 - a_1 + a_1a_3 + a_3 - 2}{(a_1 + a_3)^2 - 4} \quad (37)$$

$$S_{1111} = \frac{(a_1 + a_3 - 2)^2(4 + a_1 + 5a_3 + 2a_3^2)}{2[(a_1 + a_3)^2 - 4]^2} \quad (38)$$

$$S_{1112} = -\frac{(a_1 + a_3 - 2)^2 a_2(1 + a_3)}{2[(a_1 + a_3)^2 - 4]^2} \quad (39)$$

$$S_{1122} = \frac{(a_1 + a_3 - 2)^2(a_1 + 2a_1a_3 + a_3)}{2[(a_1 + a_3)^2 - 4]^2} \quad (40)$$

$$S_{1222} = -\frac{(a_1 + a_3 - 2)^2 a_2(1 + a_3)}{2[(a_1 + a_3)^2 - 4]^2} \quad (41)$$

$$S_{2222} = \frac{(a_1 + a_3 - 2)^2(4 + 2a_1^2 + 5a_1 + a_3)}{2[(a_1 + a_3)^2 - 4]^2} , \quad (42)$$

where

$$a_1 = 1 - \frac{2\lambda}{1 + \lambda}\sin^2 wt \quad (43)$$

$$a_2 = -\frac{2\lambda}{\sqrt{1 + \lambda^2}}\sin 2wt \quad (44)$$

$$a_3 = 1 + \frac{2\lambda}{1 - \lambda}\sin^2 wt . \quad (45)$$

The analytical solutions of $S_{ijkl}$ for simple shear flow indicate that the particle aspect ratio $a_p$ and the total shear $\gamma$ (i.e., $\gamma = c_1 t$) characterize the evolution of orientation structure. Starting from random orientation state, the $S_{ijkl}$ components as functions of total shear are shown for different particle aspect ratios in Figs. 1a–e. The periodic behaviors of $S_{ijkl}$ components originate from the tumbling of finite aspect ratio particles in simple shear flow. As illustrated in Figs. 1a–e, the period of $S_{ijkl}$ components is a strong function of aspect ratio, and as $a_p \to \infty$, the periodic behavior ceases and tensor components reach their steady values (i.e., $S_{1111} = 1$ and $S_{1112} = S_{1122} = S_{1222} = S_{2222} = 0$). Figure 1a shows that $S_{1111}$ oscillates between a maximum value and its initial value of 0.375. The maximum value of $S_{1111}$ is dependent on the aspect ratio and approach to unity as $a_p \to \infty$. If $S_{1111}$ is considered to be a measure of the degree of fiber alignment, it is obvious that the suspensions with finite aspect ratio particles never reach a perfect alignment in simple shear flow. On the other hand, all components of $S_{ijkl}$, independent of particle aspect ratio, decrease to their initial values periodically, thus indicating that the suspensions periodically form a random orientation state before attaining higher alignments in simple shear flow. As shown in Figs. 1a–e, the random orientation state does not last long, and especially high aspect ratio particles remain aligned most of the time.

### 2.2.2 Planar elongational flow

For planar elongational flows, the velocity gradient tensor is

$$u_{ij} = \begin{pmatrix} c & 0 \\ 0 & -c \end{pmatrix} , \quad (46)$$

where $c$ represents the extension rate, and from Eq. (15), $w^2$ becomes

$$w^2 = \lambda^2 c^2 . \quad (47)$$

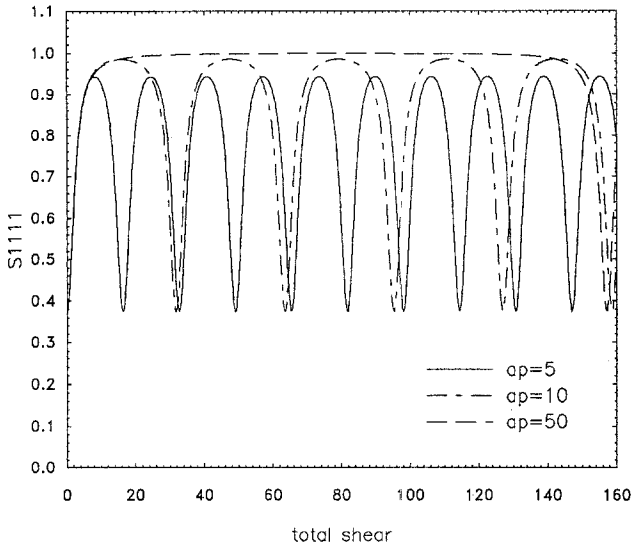


Fig. 1a. Exact solution for the fourth-order orientation tensor component $S_{1111}$ as a function of total shear for different particle aspect ratios

Since $w^2$ is always positive, the second- and fourth-order orientation tensor components for planar elongational flow simplify as

$$S_{11} = \frac{1 - a_3}{a_1 - a_3} \tag{48}$$

$$S_{12} = 0 \tag{49}$$

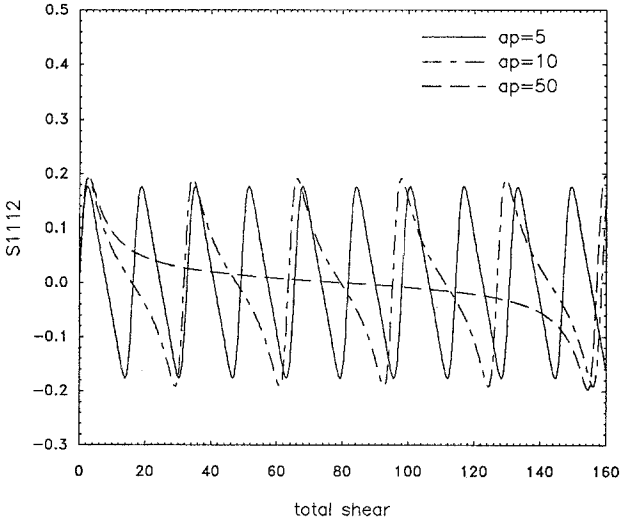


Fig. 1b. Exact solution for the fourth-order orientation tensor component $S_{1112}$ as a function of total shear for different particle aspect ratios

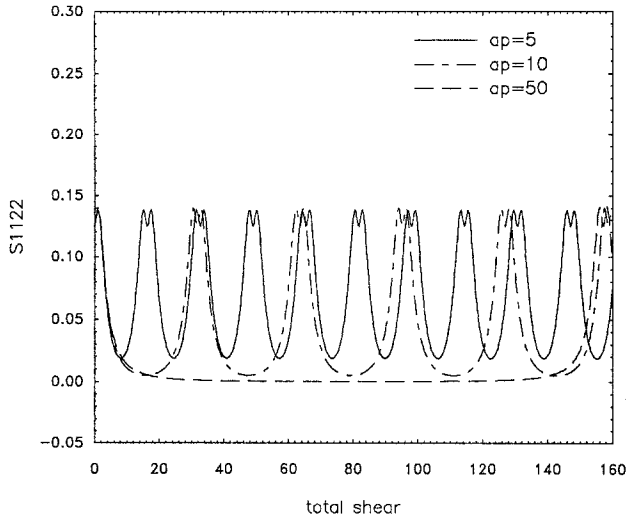


Fig. 1c. Exact solution for the fourth-order orientation tensor component $S_{1122}$ as a function of total shear for different particle aspect ratios

$$S_{22} = \frac{a_1 - 1}{a_1 - a_3} \tag{50}$$

$$S_{1111} = \frac{a_1 - 3a_3 + 2a_3^2}{2(a_1 - a_3)^2} \tag{51}$$

$$S_{1112} = 0 \tag{52}$$

$$S_{1122} = \frac{a_1 - 2a_1 a_3 + a_3}{2(a_1 - a_3)^2} \tag{53}$$

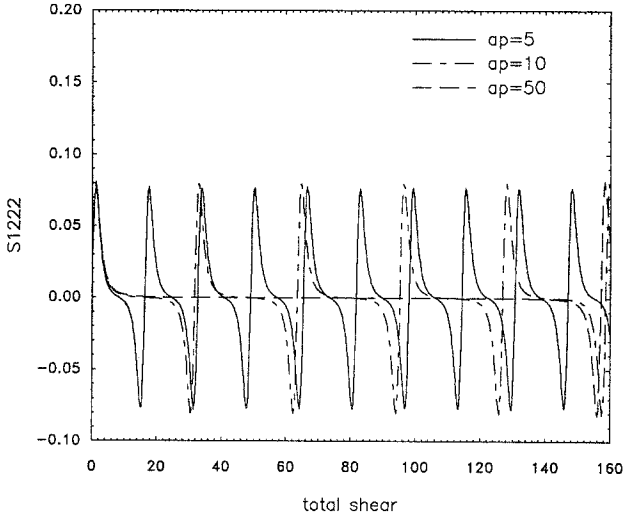


Fig. 1d. Exact solution for the fourth-order orientation tensor component $S_{1222}$ as a function of total shear for different particle aspect ratios

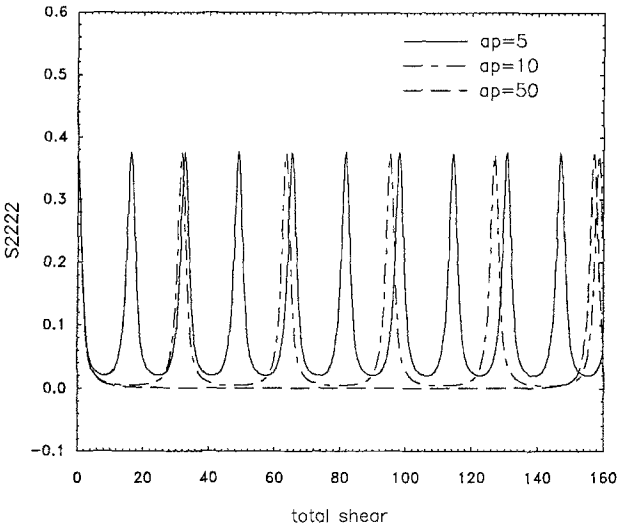


Fig. 1e. Exact solution for the fourth-order orientation tensor component $S_{2222}$ as a function of total shear for different particle aspect ratios

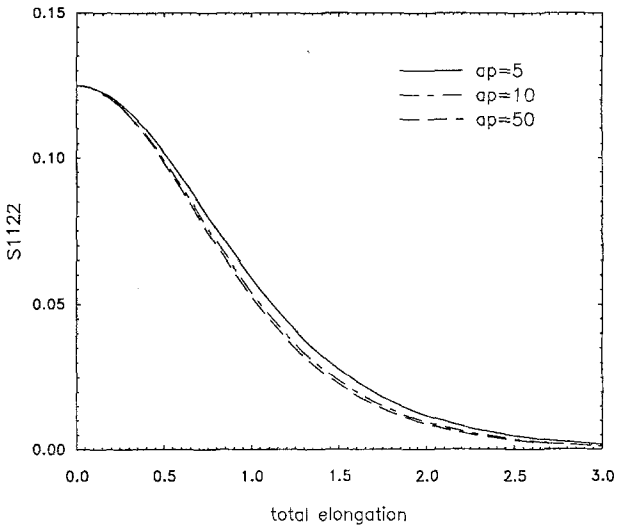


Fig. 2b. Exact solution for the fourth-order orientation tensor component $S_{1122}$ as a function of total elongation for different particle aspect ratios

$$S_{1222} = 0 \tag{54}$$

$$S_{2222} = \frac{2a_1^2 - 3a_1 + a_3}{2(a_1 - a_3)^2}\,, \tag{55}$$

where $a_1 = e^{-2\varepsilon\lambda}$; $a_2 = 0$; $a_3 = e^{2\varepsilon\lambda}$, and $\varepsilon$ is the total elongation (i.e., $\varepsilon = ct$).

The non-zero components of the fourth-order orientation tensor $S_{ijkl}$ are shown as functions of total elongation $\varepsilon$ in Figs. 2a – c. Unlike simple shear flow, the $S_{ijkl}$ components in planar elongational flow are not periodic and rapidly approach to their steady values (i.e., $S_{1111} = 1$ and $S_{1122} = S_{2222} = 0$). Moreover, Figs. 2a – c depict that particle aspect ratio in planar elongational flow does not affect the evolution of $S_{ijkl}$ components significantly.

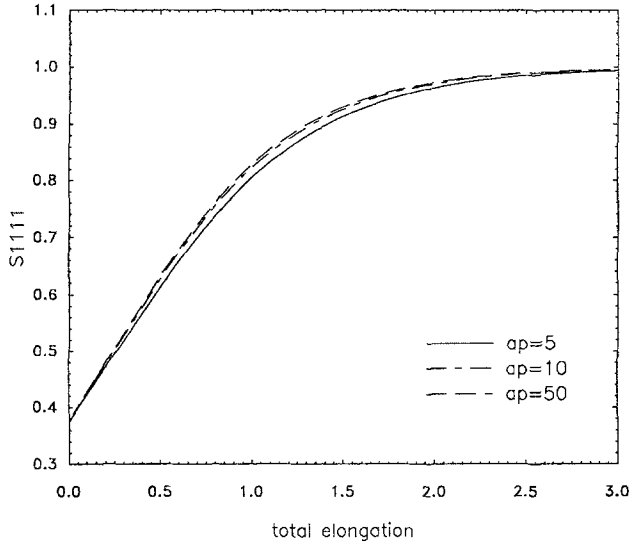


Fig. 2a. Exact solution for the fourth-order orientation tensor component $S_{1111}$ as a function of total elongation for different particle aspect ratios

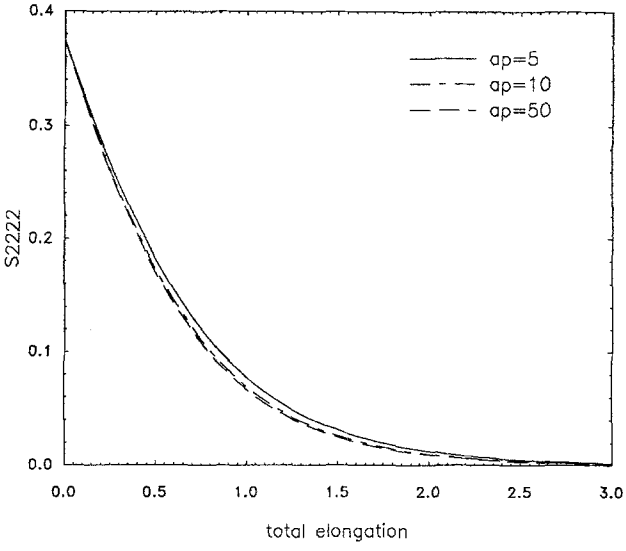


Fig. 2c. Exact solution for the fourth-order orientation tensor component $S_{2222}$ as a function of total elongation for different particle aspect ratios

## 3. Orientation evolution equations

The numerical solution of orientation distribution function is computationally intensive and not practical for complex flows. In addition, fourth-order orientation tensor $S_{ijkl}$ contains all the required information about orientation field to characterize the rheology of suspension described by Eq. (1). It should be noted that for two- and three-dimensional orientation fields, $S_{ijkl}$ has only four and 14 independent components, respectively. Hence, alternative ways are sought to evaluate tensor components without using orientation distribution function. A number of researchers have preferred to utilize evolution equations[2]) for orientation tensors which may be computationally feasible and sufficiently accurate to characterize the orientation state and the rheology of fiber suspensions. The evolution equations for orientation tensors, if used with closure approximations, can be implemented to complex flows. For such cases, the evolution equations can be solved either along particle pathlines using a Lagrangian approach, or on fixed grid points throughout the domain with an Eulerian formulation. However, the order of evolution equations as well as the order and type of closure approximations should be carefully selected for accurate results. Basic symmetry requirements inherent in the constitutive equations should also be accounted for in order to obtain consistent and meaningful descriptions.

### *3.1 Second- and fourth-order evolution equations*

As stated earlier, most constitutive models assume that the orientation of individual fibers is governed by Jeffrey's equation as given by Eq. (2). In order to obtain the orientation evolution equations, definitions of the second- and fourth-order orientation tensors are used as a starting point. Taking the derivative of Eq. (8) with respect to time and using Eq. (2), the second- and fourth-order orientation evolution equations can be written as

$$\frac{dS_{ij}}{dt} = (\Omega_{im} + \lambda \Delta_{im}) S_{mj} + (\Omega_{jm} + \lambda \Delta_{jm}) S_{mi} - 2\lambda \Delta_{kl} S_{ijkl} \tag{56}$$

$$\frac{dS_{ijkl}}{dt} = (\Omega_{im} + \lambda \Delta_{im}) S_{mjkl} + (\Omega_{jm} + \lambda \Delta_{jm}) S_{mikl} + (\Omega_{km} + \lambda \Delta_{km}) S_{mijl} + (\Omega_{lm} + \lambda \Delta_{lm}) S_{mijk} - 4\lambda \Delta_{rs} S_{ijklrs} \; . \tag{57}$$

The evolution equations given by Eq. (56) for second-order tensor $S_{ij}$ is first proposed by Hand (1960), and later by Doi (1981). The details of the mathematical manipulations are included in both publications with an accompanying proof in Doi (1981). The extension of the same idea to a higher order tensor is straightforward but cumbersome. Equation (57) represents the evolution equations for fourth-order orientation tensor $S_{ijkl}$ which potentially provide more accurate representation of the orientation structure compared to using lower order evolution equations defined by Eq. (56).

Since calculation of the orientation tensors only requires solving ordinary differential equations given in Eq. (56) or Eq. (57), the tedious computation of calculating the orientation distribution function is totally avoided. It can be easily seen that for planar orientations, three orientation equations result from Eq. (56) and five from Eq. (57). However, using $S_{ii} = 1$, the number of independent components can be reduced to two in the case of a second-order tensor and to four in the case of a fourth-order tensor. Nevertheless, these equations cannot be solved readily due to the unknowns appearing in the form of higher order tensors. Specifically, Eq. (56) contains the unknown fourth-order orientation tensor $S_{ijkl}$, while Eq. (57) contains the unknown sixth-order orientation tensor $S_{ijklrs}$. In order to solve this problem, closure approximations need to be used. With the help of these approximations, the unknown higher order terms are expressed in terms of the lower order tensors, thus forming a closed set of differential equations.

### *3.2 Closure approximations*

The idea of introducing closure approximations is first explored by Hand (1960) where the fourth-order tensor $S_{ijkl}$ is approximated by a linear combination of the second-order tensor components. The resulting closure approximation and its accuracy is studied by Hinch and Leal (1976), and later by Advani and Tucker (1987). The required tensorial symmetry for the higher order tensor is conserved when it is approx-

[2]) The terms "dynamic equations" or "equation of change" are also used to describe evolution equations.

imated by the linear closure equations. However, although the linear approximation yields exact results for random particle orientations, one can show that at higher degree of alignments the results become oscillatory and unstable for non-Brownian fibers. Corollary to this, linear closure approximations have not been considered as a viable choice for complex flows. One other alternative is to utilize quadratic closure approximation as proposed by Hinch and Leal (1976) and Doi (1981). In fact, there are a number of ways to develop similar quadratic approximations which are also referred to as decoupling approximations. The most commonly used type of quadratic approximation is

$$S_{ijkl} \simeq S_{ij} S_{kl} \ . \tag{58}$$

The popularity of Eq. (58) only arises from its simplicity despite the potential problems. Although Eq. (58) gives accurate results for aligned orientations, it violates the symmetry of $S_{ijkl}$. Specifically, Eq. (58) yields more than one possible way of approximating the identical $S_{ijkl}$ components. For example, for planar orientations, although $S_{1122}$ is identical to $S_{1212}$, approximating them with Eq. (58) and, subsequently, using them in Eq. (1) gives two different results (i.e., $S_{11}S_{22} \neq S_{12}S_{12}$). In addition, it can easily be observed that if Eq. (58) is chosen as the closure equation, it needs to be used in two different places for the simulation of complex flows of suspensions (see, for example, Eq. (4) and Eq. (6) in Rosenberg et al., 1990) which may lead to inaccurate results. In complex flows, the effects of implementing Eq. (58) in both evolution and constitutive equations are not completely known at this point. However, it is suspected that this may contribute to the divergence of the numerical results for some suspension parameters as observed by Rosenberg et al. (1990), Chiba et al. (1990) and Lee (1992). Other techniques combining the linear and quadratic closure approximations in some fashion are also available. Such composite or hybrid closure equations are investigated in detail by Hinch and Leal (1976), Altan et al. (1989), and Advani and Tucker (1987, 1990). Since the linear closure approximation as suggested by Hand (1960) yields unstable orientation dynamics for non-Brownian particles, approximations developed by combining linear and quadratic closure equations may also be susceptible to artificial oscillations as shown by Advani and Tucker (1990). In particular, for complex flows where all the velocity gradients are nonzero, the stability of the hybrid closure equations may not be assured for non-Brownian fibers. Of course, such a condition is rather difficult to identify and cannot be predicted a priori. However, some of the hybrid closure equations are shown to be useful and stable for infinite fiber aspect ratio if Brownian diffusion exists (Advani and Tucker, 1990). Recently, the inadequacies of using lower order closure equations with Eq. (56) is also addressed by Maffettone and Marrucci (1991). From this viewpoint, instead of the second-order evolution equations, higher order approximations in conjunction with Eq. (57) may be considered as an alternative and possibly more accurate approach where $S_{ijkl}$ components obtained from Eq. (57) can be directly used in Eq. (1) without additional approximation. A higher order quadratic approximation that can be used in Eq. (57) is expressed as

$$S_{ijklrs} \simeq S_{ijkl} S_{rs} \ . \tag{59}$$

Equation (59), if used with Eq. (57), conserves the tensorial symmetry for the fourth-order orientation tensor and avoids some of the shortcomings of adopting a lower order approach as explained before. Higher order evolution equations are first implemented by Altan et al. (1990) for the three-dimensional orientation predictions in Hele-Shaw flows at zero volume fraction limit. Later, Altan et al. (1992) extended this approach to non-zero particle volume fractions where the anisotropic flow of fiber suspensions in a two-dimensional straight channel is investigated. After using the fourth-order quadratic closure approximation expressed by Eq. (58) and the properties of orientation tensors defined earlier, the second-order evolution equations can be obtained as (Rao et al., 1991)

$$\frac{dS_{11}}{dt} = 2[\lambda \Delta_{11} S_{11} + (\Omega_{12} + \lambda \Delta_{12}) S_{21} - \lambda\{\Delta_{11} S_{11} + 2\Delta_{12} S_{12} + \Delta_{22} S_{22}\} S_{11}] \tag{60}$$

$$\frac{dS_{12}}{dt} = (\Omega_{21} + \lambda \Delta_{21}) S_{11} + (\Omega_{12} + \lambda \Delta_{12}) S_{22} - 2\lambda\{\Delta_{11} S_{11} + 2\Delta_{12} S_{12} + \Delta_{22} S_{22}\} S_{12} \tag{61}$$

$$\frac{dS_{22}}{dt} = 2[(\Omega_{21} + \lambda \Delta_{21}) S_{12} + \lambda \Delta_{22} S_{22} - \lambda\{\Delta_{11} S_{11} + 2\Delta_{12} S_{12} + \Delta_{22} S_{22}\} S_{22}] \ . \tag{62}$$

Similarly, with the sixth-order quadratic closure approximation expressed in Eq. (59), the resulting fourth-order evolution equations become (Rao et al., 1991).

$$\frac{dS_{1111}}{dt} = 4[\lambda A_{11} S_{1111} + (\Omega_{12} + \lambda A_{12}) S_{1112} - \lambda\{A_{11} S_{1111} + 2A_{12}(S_{1112} + S_{1222}) + A_{22} S_{2222}\} S_{1111}] \quad (63)$$

$$\frac{dS_{1112}}{dt} = 3[\lambda A_{11} S_{1112} + (\Omega_{12} + \lambda A_{12}) S_{1122}] + (\Omega_{21} + \lambda A_{21}) S_{1111} + \lambda A_{22} S_{1112} - 4\lambda[\{A_{11} S_{1111} + 2A_{12}(S_{1112} + S_{1222}) + A_{22} S_{2222}\} S_{1112}] \quad (64)$$

$$\frac{dS_{1122}}{dt} = 2[\lambda A_{11} S_{1122} + (\Omega_{12} + \lambda A_{12}) S_{1222}] + (\Omega_{21} + \lambda A_{21}) S_{1112} + \lambda A_{22} S_{1122} - 4\lambda[\{A_{11} S_{1111} + 2A_{12}(S_{1112} + S_{1222}) + A_{22} S_{2222}\} S_{1122}] \quad (65)$$

$$\frac{dS_{1222}}{dt} = \lambda A_{11} S_{1122} + (\Omega_{12} + \lambda A_{12}) S_{2222} + 3[(\Omega_{21} + \lambda A_{21}) S_{1122} + \lambda A_{22} S_{1222}] - 4\lambda[\{A_{11} S_{1111} + 2A_{12}(S_{1112} + S_{1222}) + A_{22} S_{2222}\} S_{1222}] \quad (66)$$

$$\frac{dS_{2222}}{dt} = 4[(\Omega_{21} + \lambda A_{21}) S_{1222} + \lambda A_{22} S_{2222} - \lambda\{A_{11} S_{1111} + 2A_{12}(S_{1112} + S_{1222}) + A_{22} S_{2222}\} S_{2222}] \; . \quad (67)$$

The two sets of ordinary differential equations given in Eqs. (60) – (62) and Eqs. (63) – (67) are solved separately using the public domain software Livermore Solver for Ordinary Differential Equations (LSODE). In this study, the accuracies of fourth- and sixth-order quadratic closure approximations are investigated for both finite and infinite aspect ratio particles. In the next section, predictions for simple shear and planar elongational flows are presented and compared with the analytical solutions obtained earlier.

### 3.3 Simple shear flow

For simple shear flow, the evolutions of fourth-order orientation tensor components for infinite aspect ratio particles are shown in Figs. 3a – e. The orientation state is taken to be random initially, and the tensor components are drawn as functions of total shear. In Figs. 3a – e, the analytical solutions are obtained from Eqs. (38) – (42), whereas the curves denoted by $S_{ij}$ and $S_{ijkl}$ are obtained by solving the sets of differential equations expressed in Eqs. (60) – (62) and Eqs. (63) – (67), respectively. Obviously, after Eqs. (60) – (62) are solved, the fourth-order quadratic closure approximation is used once more to determine $S_{ijkl}$ components. Hence, as mentioned before, if lower order evolution equations are used to evaluate higher order tensorial quantities, the closure approximations are needed to be implemented twice which may possibly decrease the accuracy of predictions. As shown in Figs. 3a – e, both the second- and fourth-order evolution equations yield correct asymptotic behavior. However, for the $S_{ijkl}$ components that are not initially zero, the second-order evolution equations, unlike the fourth-order, do not yield cor-

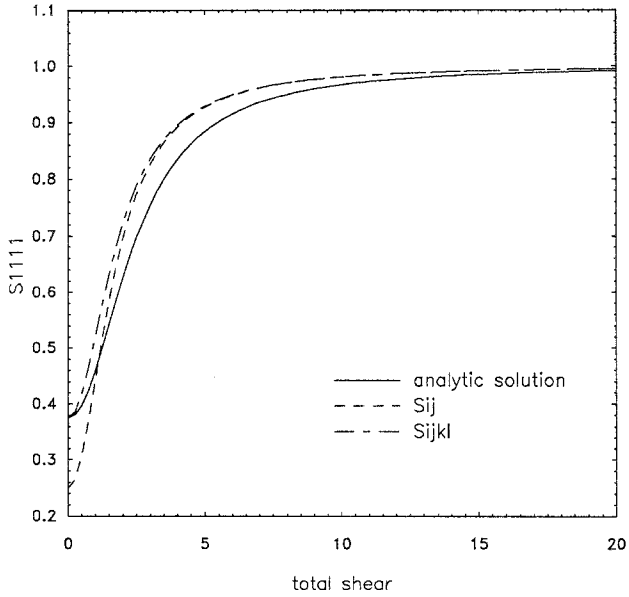


Fig. 3a. Predictions for the fourth-order orientation tensor component $S_{1111}$ as a function of total shear using second- and fourth-order orientation evolution equations with quadratic closure approximation. Particle aspect ratio = ∞

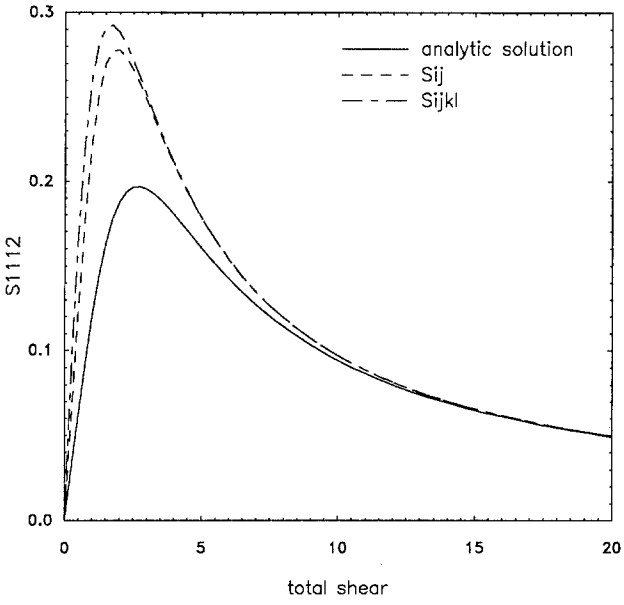


Fig. 3b. Predictions for the fourth-order orientation tensor component $S_{1112}$ as a function of total shear using second- and fourth-order orientation evolution equations with quadratic closure approximation. Particle aspect ratio = ∞

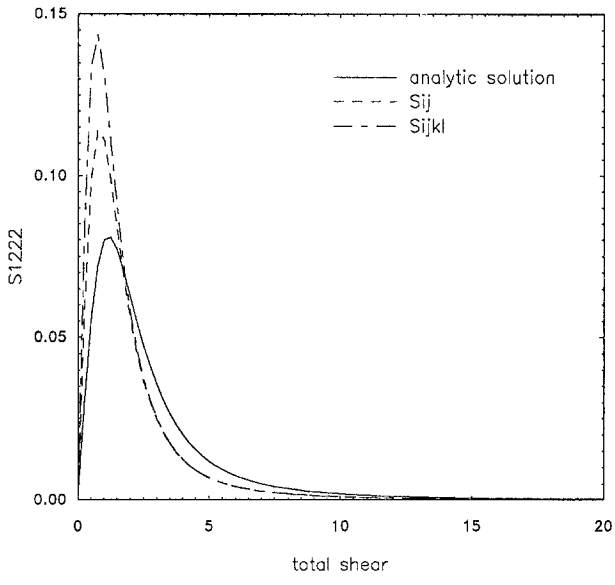


Fig. 3d. Predictions for the fourth-order orientation tensor component $S_{1222}$ as a function of total shear using second- and fourth-order orientation evolution equations with quadratic closure approximation. Particle aspect ratio = ∞

rect starting values. On the other hand, predictions from both equations quickly converge to same values which later approach to exact results asymptotically. Figure 3c illustrates three different predictions for $S_{1122}$. The curves denoted by $S_{11} \times S_{22}$ and $S_{12} \times S_{12}$ are obtained from different implementations of Eq. (58) by using the $S_{ij}$ components evaluated from Eqs. (60) – (62). Clearly, the idea of using second-order evolution equations with fourth-order quadratic approximation to predict fourth-order ten-

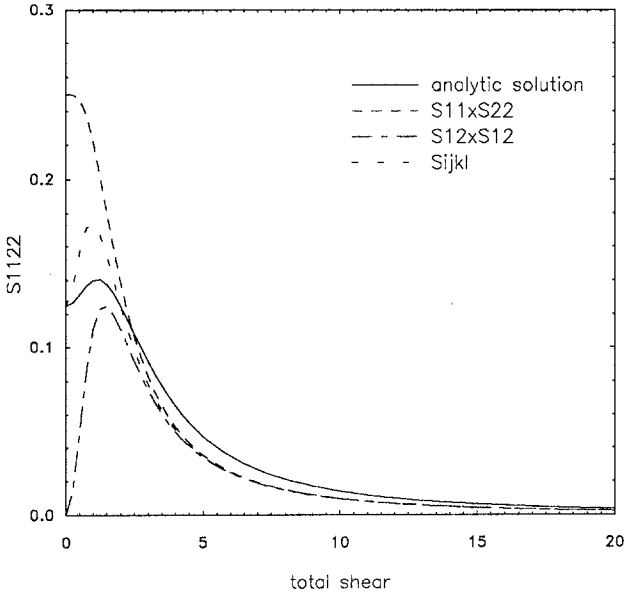


Fig. 3c. Predictions for the fourth-order orientation tensor component $S_{1122}$ as a function of total shear using second- and fourth-order orientation evolution equations with quadratic closure approximation. Particle aspect ratio = ∞

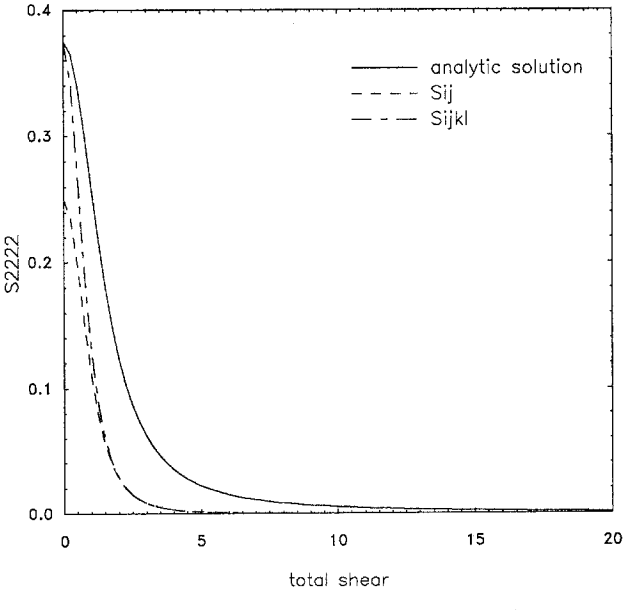


Fig. 3e. Predictions for the fourth-order orientation tensor component $S_{2222}$ as a function of total shear using second- and fourth-order orientation evolution equations with quadratic closure approximation. Particle aspect ratio = ∞

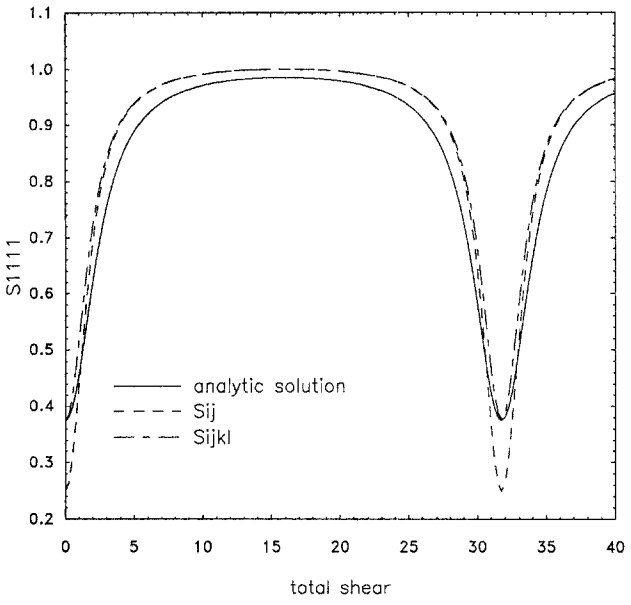


Fig. 4a. Predictions for the fourth-order orientation tensor component $S_{1111}$ as a function of total shear using second- and fourth-order orientation evolution equations with quadratic closure approximation. Particle aspect ratio = 10

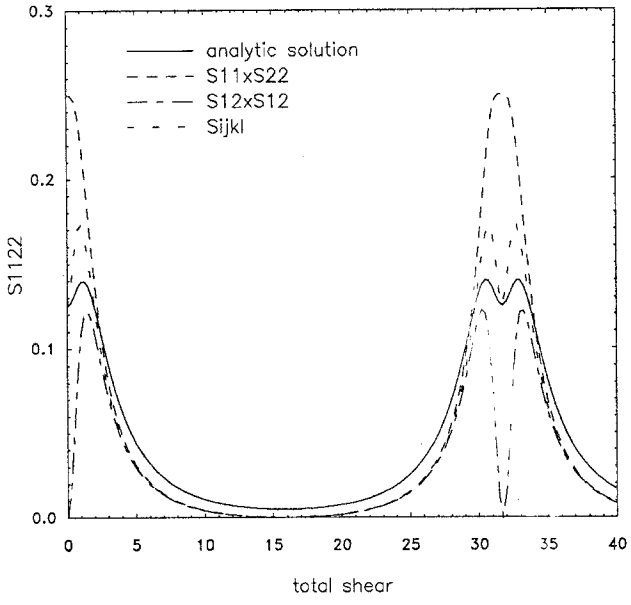


Fig. 4c. Predictions for the fourth-order orientation tensor component $S_{1122}$ as a function of total shear using second- and fourth-order orientation evolution equations with quadratic closure approximation. Particle aspect ratio = 10

sors leads to significant errors, particularly for $S_{1122}$.

In Figs. 4a–e, the evolutions of fourth-order orientation tensor components are shown for particles with an aspect ratio of 10. For finite aspect ratio particles, both the analytical solution and the predictions from evolution equations depict periodic behavior of the tensor components. Hence, as shown in the figures, the errors involved in closure approximations are also periodic. In general, the errors are most sig-

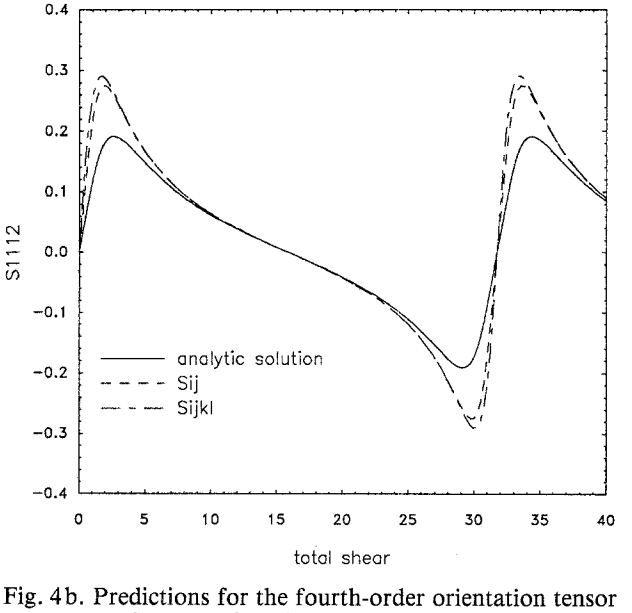


Fig. 4b. Predictions for the fourth-order orientation tensor component $S_{1112}$ as a function of total shear using second- and fourth-order orientation evolution equations with quadratic closure approximation. Particle aspect ratio = 10

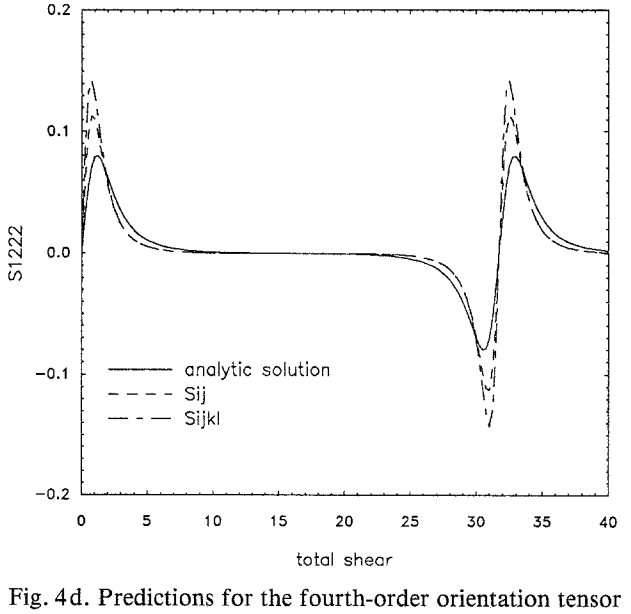


Fig. 4d. Predictions for the fourth-order orientation tensor component $S_{1222}$ as a function of total shear using second- and fourth-order orientation evolution equations with quadratic closure approximation. Particle aspect ratio = 10

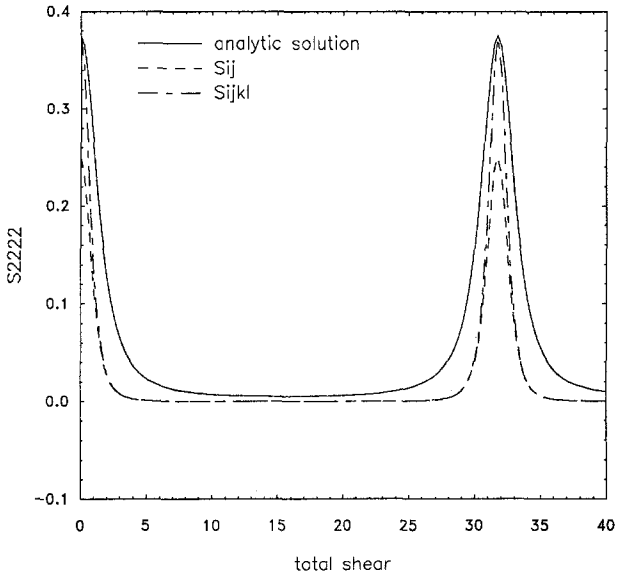


Fig. 4e. Predictions for the fourth-order orientation tensor component $S_{2222}$ as a function of total shear using second- and fourth-order orientation evolution equations with quadratic closure approximation. Particle aspect ratio = 10

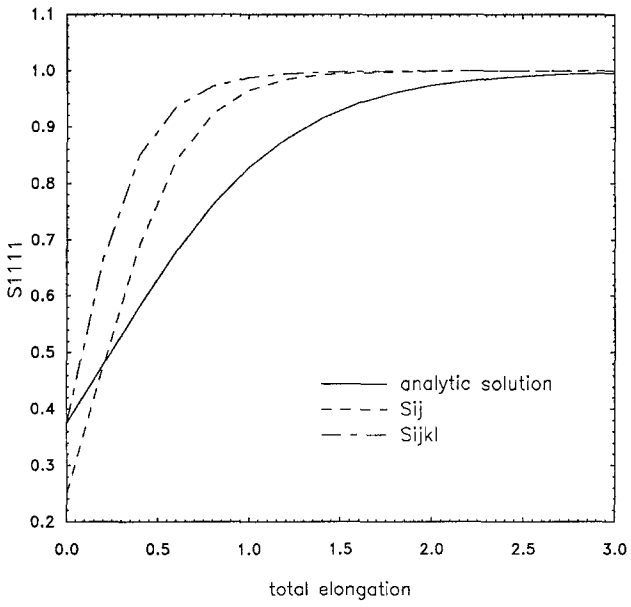


Fig. 5a. Predictions for the fourth-order orientation tensor component $S_{1111}$ as a function of total elongation using second- and fourth-order orientation evolution equations with quadratic closure approximation. Particle aspect ratio = ∞

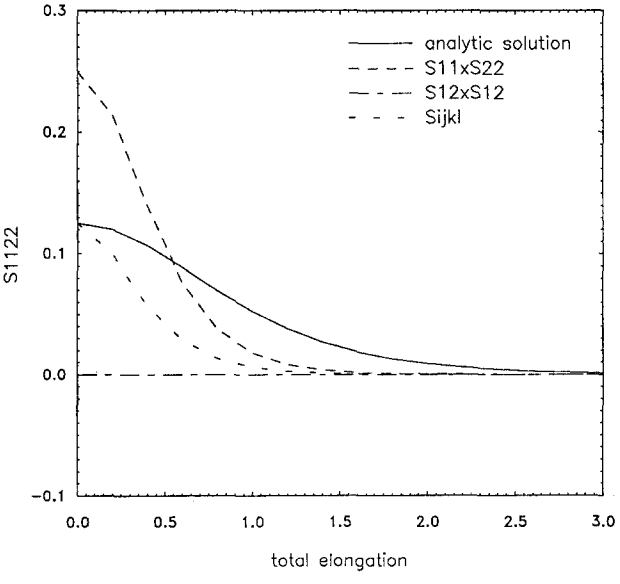


Fig. 5b. Predictions for the fourth-order orientation tensor component $S_{1122}$ as a function of total elongation using second- and fourth-order orientation evolution equations with quadratic closure approximation. Particle aspect ratio = ∞

nificant around regions where the orientation evolution is fastest (i.e., when orientation structure is rapidly passing through a random orientation distribution). It should also be pointed out that even for finite aspect ratio particles, both the second- and fourth-order evolution equations predict perfect alignment ($S_{1111} = 1$) at some point during the oscillatory behavior of orientation structure. Such a prediction, as shown by analytical results, is not correct since orientation structure formed by finite aspect ratio fibers never displays a perfect alignment. Hence, the errors induced by using quadratic closure approximations become particularly significant for low aspect ratio particles.

### *3.4 Planar elongational flow*

The evolution of non-zero components of the fourth-order orientation tensor for infinite aspect ratio particles in planar elongational flow is shown in Figs. 5a–c. Starting from a random orientation field, the preferred orientation is always along the flow direction, thus yielding only three non-zero $S_{ijkl}$ components. The evolution of orientation structure is not periodic for both finite and infinite aspect ratio particles. Since the second- and fourth-order evolution equations are found to depict similar characteristics for all particles, the results for finite aspect ratio particles are not included. As in the case of simple shear flow, the predictions from second-order evolution equations start from incorrect values for all $S_{ijkl}$ components. Moreover, as shown in Fig. 5b, $S_{1122}$ can erroneously be determined as zero by using

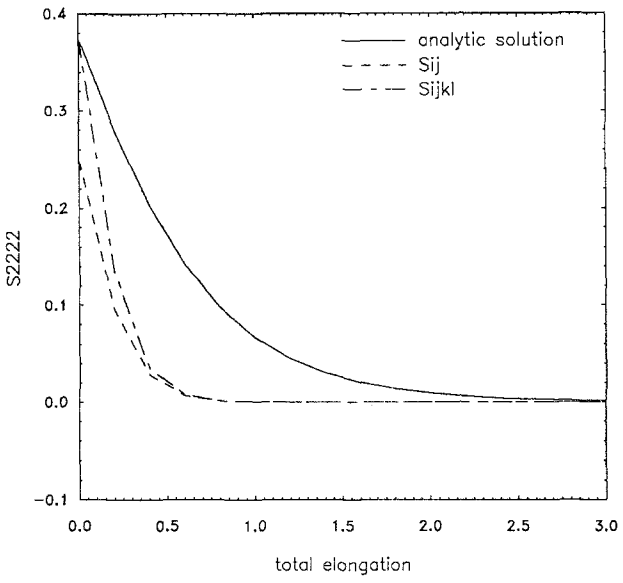


Fig. 5c. Predictions for the fourth-order orientation tensor component $S_{2222}$ as a function of total elongation using second- and fourth-order orientation evolution equations with quadratic closure approximation. Particle aspect ratio = $\infty$

$S_{12} \times S_{12}$, which illustrates the possibility of inconsistent approximations for identical $S_{ijkl}$ components. On the other hand, results from both equations asymptotically approach to correct $S_{ijkl}$ values.

### 3.5 *A simple example: planar Poiseuille flow*

The analytical solutions of orientation evolution can also be determined for a class of non-homogeneous flows at zero volume fraction limit. The exact expressions for the rotation of a particle and for the orientation distribution function can be derived for both two- and three-dimensional flows and orientation fields, if the form of velocity gradient tensor does not change along particle pathlines. Hence, for such complex flows, the accuracies of closure approximations can be analyzed throughout the flow domain (i.e., Eulerian representation) by solving the components of orientation tensors using orientation evolution equations along particle pathlines.

A simple example is the planar Poiseuille flow through a channel as shown in Fig. 6a. The randomly oriented particles are assumed to be introduced into the fully developed velocity profile at $x = 0$. If the half channel width is taken to be unity (i.e., $y = 1$ at the channel wall), the parabolic velocity profile can be expressed as

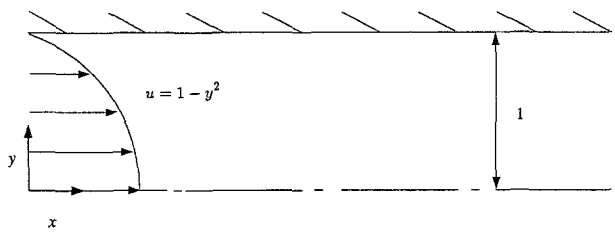


Fig. 6a. The planar channel geometry and flow parameters

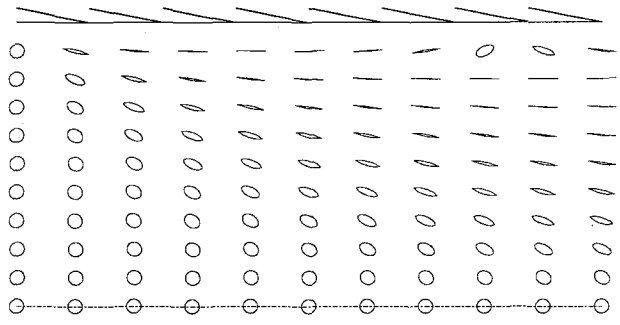

Fig. 6b. The analytic solutions of $S_{ij}$ components represented by ellipses in planar Poiseuille flow

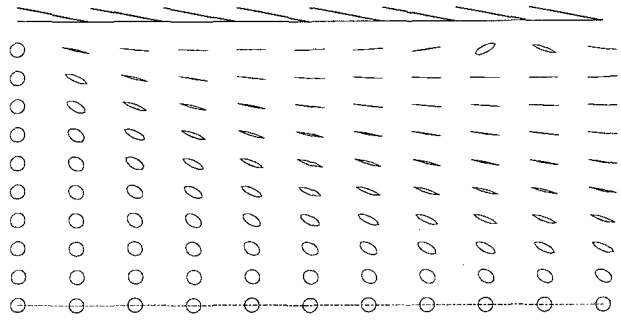

Fig. 6c. The $S_{ij}$ components obtained from the second-order evolution equations with quadratic closure approximation in planar Poiseuille flow

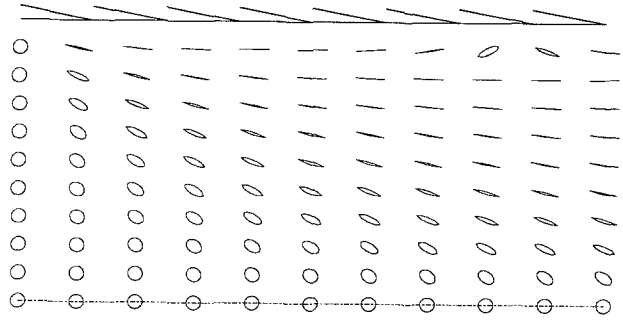

Fig. 6d. The $S_{ij}$ components obtained from the fourth-order evolution equations with quadratic closure approximation in planar Poiseuille flow

$$u = 1 - y^2 \ . \tag{62}$$

The only non-zero velocity gradient is the shear rate $c_1$, and therefore, simple shear flow equations (35) – (45) can be utilized with $wt$ defined as

$$wt = -\frac{yx}{1-y^2}\sqrt{1-\lambda^2} \ . \tag{63}$$

Figures 6b – d depict the orientation field represented by ellipses which are evaluated from the second-order orientation tensors. The fiber aspect ratio is taken to be 10 and random fiber orientation at the inlet is shown as circles. Although the actual ratio of channel length to half channel width (i.e., aspect ratio of the computational flow domain) is four, the channel width is stretched in Figs. 6b – c for clarity. Figure 6b represents the analytical solution; whereas, Fig. 6c and d are obtained from the evolution expressions given in Eqs. (60) – (62) and Eqs. (63) – (67), respectively. It should be noted that although the use of second-order tensor is not convenient for rheological characterization, its graphical representation throughout the flow domain illustrates some of the important physical aspects. Moreover, if the flow contains too few particles to affect the flow behavior, then practically, one only needs to determine $S_{ij}$ components for the complete orientation characterization. Therefore, for the second-order orientation tensor, it is more useful to concentrate on the degree of alignment and maximum orientation angle predictions as opposed to individual tensor components. A careful review of Figs. 6b – d shows that the maximum orientation angles are accurately predicted by both the second- and fourth-order evolution equations. However, the degree of alignments, as illustrated by the degree of deformation of orientation ellipses, differ considerably in regions where particles are moderately aligned.

From this viewpoint, Tables 1 and 2 present the accuracies of evolution equations characterized by the maximum orientation angles and degree of alignments for particles with aspect ratio infinity and 10, respectively. Both tables show that the exact maximum orientation angle values are predicted by both evolution equations. The same behavior is also observed in numerous other homogeneous flows. On the other hand, the degree of alignments are not determined accurately at low total shears. In fact, surprisingly, the degree of alignments obtained from fourth-order equations are found to be slightly worse than the ones obtained from second-order evolution equations. Therefore, if only $S_{ij}$ components are needed, the use of fourth-order evolution equations is not justified. However, as described earlier, fourth-order evolution equations provide significant improvements for the prediction of $S_{ijkl}$ values.

## 4. Concluding Remarks

The analytical expressions for the evolution of planar orientation structure which is characterized by tensorial quantities are presented for dilute particle suspensions subjected to two-dimensional arbitrary homogeneous flow fields. The general analytical expressions are simplified for simple shear and planar elongational flows, which are later used to evaluate the accuracies of commonly used orientation evolu-

Table 1. The degree of alignments and maximum orientation angles in shear flows for infinite aspect ratio particles

| Total shear $\gamma$ | Analytical results | | Second-order evolution equations: $\frac{dS_{ij}}{dt}$ | | Fourth-order evolution equations: $\frac{dS_{ijkl}}{dt}$ | |
|---|---|---|---|---|---|---|
| | $\lambda_1$ | $\phi_{max}$ | $\lambda_1$ | $\phi_{max}$ | $\lambda_1$ | $\phi_{max}$ |
| 1.0 | 0.7236 | 31.7175 | 0.8727 | 31.7175 | 0.9375 | 31.7175 |
| 2.0 | 0.8536 | 22.5000 | 0.9714 | 22.5000 | 0.9895 | 22.5000 |
| 3.0 | 0.9160 | 16.8450 | 0.9917 | 16.8450 | 0.9971 | 16.8450 |
| 4.0 | 0.9472 | 13.2825 | 0.9969 | 13.2825 | 0.9990 | 13.2825 |
| 5.0 | 0.9642 | 10.9007 | 0.9986 | 10.9007 | 0.9995 | 10.9007 |
| 6.0 | 0.9743 | 9.2175 | 0.9993 | 9.2175 | 0.9998 | 9.2175 |
| 7.0 | 0.9808 | 7.9727 | 0.9996 | 7.9727 | 0.9999 | 7.9727 |
| 8.0 | 0.9851 | 7.0181 | 0.9998 | 7.0181 | 0.9999 | 7.0181 |
| 9.0 | 0.9881 | 6.2644 | 0.9999 | 6.2644 | 1.0000 | 6.2644 |
| 10.0 | 0.9903 | 5.6550 | 0.9999 | 5.6550 | 1.0000 | 5.6550 |

Table 2. The degree of alignments and maximum orientation angles in shear flows for particle aspect ratio $a_p = 10$

| Total shear $\gamma$ | Analytical results | | Second-order evolution equations: $\frac{dS_{ij}}{dt}$ | | Fourth-order evolution equations: $\frac{dS_{ijkl}}{dt}$ | |
|---|---|---|---|---|---|---|
| | $\lambda_1$ | $\phi_{max}$ | $\lambda_1$ | $\phi_{max}$ | $\lambda_1$ | $\phi_{max}$ |
| 2.0 | 0.8488 | 22.3111 | 0.9693 | 22.3111 | 0.9887 | 22.3111 |
| 4.0 | 0.9429 | 12.6707 | 0.9964 | 12.6707 | 0.9988 | 12.6707 |
| 6.0 | 0.9703 | 8.1697 | 0.9991 | 8.1697 | 0.9997 | 8.1697 |
| 8.0 | 0.9810 | 5.5279 | 0.9996 | 5.5279 | 0.9999 | 5.5279 |
| 10.0 | 0.9860 | 3.7016 | 0.9998 | 3.7016 | 0.9999 | 3.7016 |
| 12.0 | 0.9885 | 2.2786 | 0.9999 | 2.2786 | 1.0000 | 2.2786 |
| 14.0 | 0.9898 | 1.0591 | 0.9999 | 1.0591 | 1.0000 | 1.0591 |
| 16.0 | 0.9900 | −0.0758 | 0.9999 | −0.0758 | 1.0000 | −0.0758 |
| 18.0 | 0.9897 | −1.2166 | 0.9999 | −1.2166 | 1.0000 | −1.2166 |
| 20.0 | 0.9883 | −2.4555 | 0.9999 | −2.4555 | 1.0000 | −2.4555 |

tion equations with quadratic closure approximations. Specifically, importance of the order of closure approximations and evolution equations is examined. Although the second-order orientation evolution equations with quadratic closure approximations have been used most often for complex flows, a number of significant limitations are found regarding the determination of the components of fourth-order orientation tensor. First, when the particles are initially in random orientation, the starting values for non-zero tensor components are not correctly predicted with the fourth-order quadratic closure equations. Second, after solving the second-order evolution equations, the implementation of the fourth-order quadratic closure approximation is shown to yield different results for the approximation of some of the identical fourth-order tensor components. These two important shortcomings can be avoided by using the fourth-order evolution equations with a sixth-order quadratic closure approximation. However, for the prediction of second-order orientation tensor, the second-order evolution equations performed slightly better compared to fourth-order equations. It is also found that for all aspect ratios and flow cases, the correct preferred orientation direction is predicted by both the second- and the fourth-order evolution equations with quadratic closures; whereas, the degree of alignment which is described by the maximum eigenvalue of the second-order tensor is not determined accurately by using both evolution equations.

## References


Advani SG, Tucker CL III (1987) The use of tensors to describe and predict fiber orientation in short fiber composites. J Rheology 31 (8):751 – 784

Advani SG, Tucker CL III (1990) Closure approximations for three-dimensional structure tensors. J Rheology 34 (3):367 – 386

Akbar S, Altan MC (1992) On the solution of fiber orientation in two-dimensional homogeneous flows. Polym Eng Sci 32(12):810 – 822

Altan MC (1990) A review of fiber-reinforced injection molding: flow kinematics and particle orientation. J Thermoplastic Composite Materials 3:275 – 313

Altan MC, Subbiah S, Güçeri Sİ, Pipes RB (1990) Numerical prediction of three-dimensional fiber orientation in hele-shaw flows. Polym Eng Sci 30:848 – 859

Altan MC, Güçeri Sİ, Pipes RB (1992) Anisotropic channel flow of fiber suspensions. J Non-Newtonian Fluid Mech 42:65 – 83

Altan MC, Advani SG, Güçeri Sİ, Pipes RB (1989) On the description of the orientation state for fiber suspensions in homogeneous flows. J Rheology 33 (7):1129 – 1155

Batchelor GK (1970) The stress system in a suspension of force-free particles. J Fluid Mech 41 (3):545 – 570

Bretherton FP (1962) The motion of rigid particles in a shear flow at low Reynolds number. J Fluid Mech 14:284 – 304

Chiba K, Nakamura K, Boger DV (1990) A numerical solution for the flow of dilute fiber suspensions through an axisymmetric contraction. J Non-Newtonian Fluid Mech 35:1 – 14

Dinh SM, Armstrong RC (1984) A rheological equation of state for semiconcentrated fiber suspensions. J Rheology 28 (3):207 – 227

Doi M (1981) Molecular dynamics and rheological properties of concentrated solutions of rodlike polymers in isotropic and liquid crystalline phases. J Polym Sci, Polym Phys Ed 19:229 – 243

Ericksen JL (1960) Transversely isotropic fluids. Kolloid-Z 173:117 – 122

Evans JG (1975) The flow of a suspension of force-free rigid rods in a Newtonian fluid. Ph D thesis, Cambridge University

Folgar F, Tucker CL III (1984) Orientation behavior of fibers in concentrated suspensions. J Reinforced Plastics and Composites 3:98 – 119

Hand GL (1962) A theory of anisotropic fluids. J Fluid Mech 13:33 – 46

Hinch EJ, Leal LG (1976) Constitutive equations in suspension mechanics. Part 2. Approximate forms for a suspension of rigid particles affected by Brownian rotations. J Fluid Mech 76 (1):187 – 208

Hinch EJ, Leal LG (1975) Constitutive equations in suspension mechanics. Part 1. General formulation. J Fluid Mech 71 (3):481 – 495

Jeffrey GB (1922) The motion of ellipsoidal particles immersed in a viscous fluid. Proc Royal Soc (London) A 102:161 – 179

Keunings R (1989) Simulation of viscoelastic fluid flow, in Tucker CL III (ed) Computer modeling for polymer processing. Carl Hanser Verlag

Lee SJ (1992) Numerical study on three-dimensional flow of fiber suspensions. Ph D thesis, Seoul National University

Lipscomb GG, Denn MM, Hur DU, Boger DV (1988) The flow of fiber suspensions in complex geometries. J Non-Newtonian Fluid Mech 26:297 – 325

Maffettone PL, Marrucci G (1991) A two-dimensional approach to the constitutive equation of nematic polymers. J Non-Newtonian Fluid Mech 38:273 – 288

Malamataris N, Papanastasiou TC (1991) Closed-form material functions for semidilute fiber suspensions. J Rheology 35 (3):449 – 464

Papanastasiou TC, Alexandrou AN (1987) Isothermal extrusion of non-dilute fiber suspensions. J Non-Newtonian Fluid Mech 25:313 – 328

Phan-Thien N, Graham AL (1991) A new constitutive model for fibre suspensions: flow past a sphere. Rheol Acta 30:44 – 57

Rao BN, Akbar S, Altan MC (1991) A comparative study on the solution techniques for fiber orientation in two-dimensional converging and diverging flows. J Thermoplastic Composite Materials 4:311 – 348

Rosenberg J, Denn M, Keunings R (1990) Simulation of non-recirculating flows of dilute fiber suspensions. J Non-Newtonian Fluid Mech 37:317 – 345

Stover CA, Koch DL, Cohen C (1992) Observations of fibre orientation in simple shear flow of semi-dilute suspensions. J Fluid Mech 238:277 – 296

Szeri AJ, Leal LG (1992) A new computational method for the solution of flow problems of microstructured fluids. J Fluid Mech 242:549 – 576

Tucker CL III (1991) Flow regimes for fiber suspensions in narrow gaps. J Non-Newtonian Fluid Mech 39:239 – 268

(Received June, 24 1992;
accepted December, 16 1992)

For correspondence:

Prof. M. Cengiz Altan
School of Aerospace and Mechanical Engineering
University of Oklahoma
Norman, OK 73019, USA